Contents lists available at ScienceDirect

Fuel

journal homepage: www.elsevier.com

Full Length Article

Interaction of diesel engine soot with NO_2 and O_2 at diesel exhaust conditions. Effect of fuel and engine operation mode

María Abián[a], Cristina Martín[a], Pablo Nogueras[a], Jesús Sánchez-Valdepeñas[b], José Rodríguez-Fernández[b], Magín Lapuerta[b], María U. Alzueta[a,*]

[a] Aragón Institute of Engineering Research (I3A), Department of Chemical and Environmental Engineering, University of Zaragoza, 50018 Zaragoza, Spain
[b] Escuela Técnica Superior de Ingenieros Industriales, University of Castilla-La Mancha, 13071 Ciudad Real, Spain

ARTICLE INFO

Keywords:
Diesel soot
Soot reactivity
Nitrogen oxides
NO_2
Diesel engine
Alternative diesel fuels

ABSTRACT

This work shows a study of the reactivity of twelve different types of soot with either NO_2 or O_2 under reacting conditions typically present in diesel particulate filters (DPFs). The soot samples were obtained from the combustion of four conventional and alternative fuels (diesel, biodiesel and two paraffinic fuels) in a diesel engine bench operated under three different engine operation modes: a typical urban-driving mode and two variations to this mode to assess the effect of the injection settings. The main objective of the work is to relate the oxidative reactivity of the soot to the nature and the origin of each sample. The possible simultaneous elimination of soot and NO_x at typical diesel exhaust conditions is examined, as well. The reactivity tests were performed in a laboratory quartz gas flow reactor, discontinuous for the solid. The soot-NO_2 interaction was studied with 200 ppm of NO_2 at 500 °C and the soot-O_2 interaction was studied with 5% O_2 at 500 °C and 600 °C. The experimental results were used to determine the time needed for the complete conversion of carbon (τ) through the use of the equations of the Shrinking Core Model for solid-gas reactions with decreasing size particle and chemical reaction control. In general, the τ values show that the diesel fuel generates a less reactive soot than biodiesel or the alternative paraffinic fuels. In addition, increasing the injection pressure or adding a post-injection to the original injection strategy generates a more reactive soot. These findings point out that there is potential to achieve efficient regeneration processes in DPFs through other fuels than conventional ones and via engine calibration.

1. Introduction

Particulate matter (including soot) originated in combustion has been largely investigated because of its effect on the environment and human health (carcinogenicity [1], climate changes [2]). Among the different soot sources, diesel engines appear to be one of the most important ones, both because of their contribution compared to other engines and because of the spread of these combustion sources. The most recent legislation, Euro 6, imposes that almost all soot mass must be removed from the diesel exhaust, forcing vehicle manufacturers to incorporate particle filters in their new models. Limits to the particulate matter emitted by gasoline direct injection (GDI) vehicles have been introduced, as well [3]. Therefore, the interest of soot characterization has moved toward its effect on the processes occurring in particulate filters. Sufficient filtering efficiency must be achieved, and at the same, time the fuel penalty must be reduced as much as possible. Catalyzed filter substrates should enable the oxidation of soot under O_2-containing gases at temperatures around 500–600 °C (typically achieved under active regeneration strategies), in this context, the role of NO_2 on soot oxidation has been explored.

Soot oxidation with nitrogen dioxide occurs at lower temperature than oxygen-assisted regeneration [4,5]. In the usual diesel exhaust temperature range, passive filter regeneration (i.e. no additional fuel is injected to increase the filter temperature) is possible, as long as NO_2 concentration is enough [6]. Active regeneration only occurs if the pressure drop across the filter is higher than a threshold and leads to a decrease in fuel economy. Nevertheless, engine-out NO_2 concentration is usually insufficient, and therefore, an oxidation catalyst upstream of the filter is needed to convert NO to NO_2 [7].

* Corresponding author.
Email address: uxue@unizar.es (M.U. Alzueta)

https://doi.org/10.1016/j.fuel.2017.10.025
Received 19 June 2017; Received in revised form 31 August 2017; Accepted 5 October 2017
Available online xxx
0016-2361/

The influence of NO_2 on the formation of soot surface oxygenated functionalities has been investigated [8–10]. It has been hypothesized that an initial step for soot oxidation is the chemisorption of oxygen atoms on the graphene layers [9]. This step is enhanced in the presence of NO_2 due to the lower dissociation energy compared to that of O_2 [10]. The oxidation mechanism and the reaction products are different when soot oxidation progresses under a NO_2-containing atmosphere. In this case, the soot-NO_2 interaction can produce species such as NO, HONO and N_2O [11–13]. Apart from NO_2, NO may interact with soot presumably at higher temperatures, at least above 600 °C [9].

In this work, twelve soot samples generated in a 4 cylinder automotive diesel engine were subjected to reactivity tests with NO_2 and O_2 at diesel exhaust conditions. The engine was run with four types of fuels (conventional diesel, and three alternative fuels, referred to as biodiesel, GTL "Gas-to-Liquid" fuel and HVO "Hydrogenated Vegetable Oil" fuel) under three stationary engine operation modes: a typical urban mode using the original calibration implemented in the Electronic Control Unit, and two modifications of the injection parameters. Both soot-NO_2 and soot-O_2 interactions were examined in a laboratory quartz gas flow reactor and the effect of the origin of the different soot samples was analyzed. To this end, the time needed for the complete conversion of carbon (τ) was determined. In addition, thermogravimetric analyses were made to support the discussion of results.

Table 1
Diesel engine specifications.

Fuel injection system	DI, common-rail
Number of cylinders	4
Valves	16
Bore (mm)	84
Stroke (mm)	90
Compression ratio	16:01
Displacement (cm^3)	1994
Maximum power (kW)	111 (at 4000 rpm)
Maximum torque (Nm)	323 (at 2000 rpm)

2. Experimental

A 4-cylinder, 4-stroke, turbocharged, Euro 5 Nissan diesel engine, model M1D, was run to generate to soot samples. This engine is equipped with a high pressure-cooled EGR loop, an oxidation catalyst (DOC) and a diesel particle filter (DPF). The main specifications of the engine are listed in Table 1. The engine bench is fitted with sensors for measuring and recording temperature and pressure in critical locations (intake air, fuel, exhaust gases, lube oil). INCA PC software and ETAS ES 591.1 hardware were used for the communication with the engine electronic control unit (ECU), and for setting the injection pressure and the injection strategy, as described later. More details of this installation can be found in previous works [14,15].

A by-pass line was installed in the exhaust configuration (Fig. 1) to collect the soot in a cylindrical shell filled with stainless steel mesh as filtering medium. After every experiment, the shell is disassembled and the soot separated for subsequent analysis. The collection method has been detailed and validated in previous works [16].

The soot reactivity experiments were carried out in an experimental installation specifically designed for addressing gas-carbon material reactions (see previous research works: e.g. [17–19]).

The laboratory installation is constituted by a quartz tubular reactor of 15 mm inside diameter and with a bottle neck in the middle where a quartz wool plug is placed. The reactor is placed inside of an electrically heated oven to control the reaction temperature. In each batch, the reactor is filled with a mixture of around of 5 mg of soot and 350 mg of silica, which is deposited over the plug, resulting in a thin layer. Silica is used to facilitate the introduction of the soot samples into the reactor and to prevent soot particles agglomeration. The temperature controller of the oven is connected to a thermocouple located just under the quartz wool plug. The heating of the reaction system up to each reaction temperature is performed in an inert N_2 atmosphere at 10 °C/min. Once the desired temperature is reached, the reactant gaseous mixture is fed into the reactor, replacing the N_2 flow. All the gases are fed through mass flow controllers from gas cylinders. It is important to indicate that this is a batch process for the solid and continu-

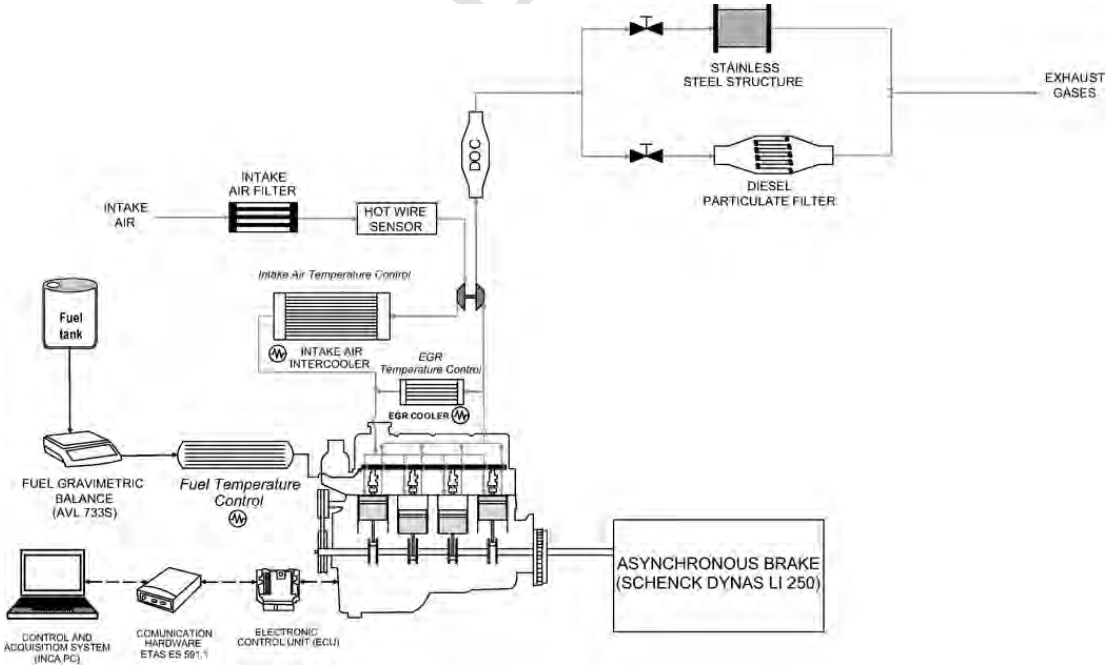

Fig. 1. Engine exhaust configuration.

ous to the reactant gas. Therefore, the initial amount of soot is progressively consumed as the reaction proceeds, whereas the total reactant gas flow is kept constant throughout the experiment. The experiments performed include the interaction of soot with 200 ppm (nominal concentration) NO_2 at 500 °C, and the interaction of soot with 5% (nominal concentration) O_2 at 500 and 600 °C. For the tests, the raw soot samples are used; i.e. without any pre-treatment. However, the heating up of the soot sample in the reaction zone to the reaction temperature in a N_2 atmosphere can be considered as a conditioning treatment inherent to the experimental procedure that removes any absorbed volatiles within the soot structure under the conditions reached.

The reaction products at the reactor outlet are cooled down by means of external refrigeration with air and analyzed as function of the reaction time (every 5–10 s). The gas products analyzing system is constituted by a continuous infrared (IR) CO/CO_2 analyzer and a chemiluminescence $NO_x/NO_2/NO$ analyzer. The estimated uncertainties of the measurements are ±5%.

The general uncertainty in the results reports an agreement within 8% in the subsequently determined time for the complete conversion of carbon.

3. Test matrix

In the present work, the soot samples analyzed were generated from the combustion of four different fuels. The first one is fossil diesel fuel that meets the EN-590 Standard with no biodiesel content. It was donated by Repsol Corporation (Spain). Paraffinic HVO fuel was produced by Neste (Finland) through hydro-treating of a blend of vegetable oils, and subsequent isomerization to improve the cold flow properties. GTL was produced by Sasol Corporation through a low temperature Fischer Tropsch process (LTFT), and represents a different route for obtaining paraffinic diesel fuels. Although natural gas was the feedstock for GTL, the properties of the used fuel are common to fuels produced through Fischer-Tropsch process from renewable feedstock (BTL, biomass-to-liquid). Finally, a biodiesel fuel (EN-14214) derived from animal fats and supplied by Stock del Vallés (Spain) was used. Table 2 presents the main properties of all the used fuels.

A single operation mode (denoted in his work as U9 and selected from the New European Driving Cycle, after a conversion process into stationary modes following the procedure described in [20] is considered as base case). U9 mode is characterized by a high particulate matter emission and low exhaust temperature. Therefore, this mode represents typical exhaust conditions during the soot loading period in a DPF. The working parameters of U9 mode, according to the original engine calibration, are shown in Table 3.

Table 2
Fuel properties.

Properties	Diesel	HVO	GTL	Biodiesel
Density at 15 °C (kg/m^3)	811	779.6	774	874.3
Viscosity at 40 °C (mm^2/s)	2.02	2.99	2.34	4.5
Lubricity (WS1.4) (μm)	226	334	211	187
Lower heating value (MJ/kg)	43.04	43.96	44.03	37.26
CFPP (°C)	−30	−21	−7	9
Aromatic content (% w/w)	17.2	0	0	0
Cetane number	67	94.8	89.2	68.8
Acid number	0.16	0.06	0.20	0.34
Sulfur (mg/kg)	<10	<10	<10	<10
Water (mg/kg)	60	19.2	20	102
C (% w/w)	85.74	85.36	84.82	76.45
H (% w/w)	14.26	14.64	15.18	12.36
O (% w/w)	0	0	0	11.19

Table 3
Operation mode parameters – U9 mode.

Speed (rpm)	1667
Effective torque (Nm)	78
EGR ratio (%)	22
Injection strategy	Split, pilot + main
Start of pilot injection (°CA aTDC)	−12.7
Start of main injection (°CA aTDC)	5
Injection pressure (bar)	660

Small variations were introduced in the injection settings of this mode to explore their effect on the soot characteristics. First, injection pressure was increased up to 720 bar, 10% higher than the original setting in U9 mode (here denoted as 'U9 + p_{inj}'). Increasing injection pressure for improving fuel atomization is a tendency in road transport at present. Second, one post injection (61 °CA aTDC, 2.59 μL/inj) was added to the U9 injection strategy (here denoted as 'U9 + post'). This is a current injection trend for improving the performance of after-treatment techniques, by increasing engine-out temperature.

4. Interpretation of soot reactivity results

To measure the reactivity of the different soot samples, the time needed for the complete conversion of carbon (τ) was used. The Shrinking Core Model (SCM) with decreasing size particle and reaction control was used to calculate τ. The SCM include mathematical developments and characteristic equations (see Levenspiel [21] for a detailed description), and allows to relate the time needed for the complete conversion of carbon, τ, and the carbon conversion at any time *t*, X_c, through Eq. (1).

$$\frac{t}{\tau} = 1 - (1 - X_c)^{1/3} \tag{1}$$

In Eq. (1), the conversion of carbon at any time *t*, X_c, is calculated as the weight of carbon reacted in the experiment (W_C) related to the initial weight of carbon (W_{C_0}), trough Eq. (2):

$$X_C = \frac{W_{C_0} - W_C}{W_{C_0}} \tag{2}$$

The procedure and equations used to determine W_C and W_{C_0} are described as follows.

Literature results establish that, in both cases (soot-O_2 and soot-NO_2 interaction), the carbon in soot is converted into CO and CO_2 (see for instance [22] for soot-O_2 and [10] for soot-NO_2). Thus, in the present work, considering the concentration profiles of CO and CO_2 with time, the carbon weight remaining within the reactor at any time (W_C) was calculated through Eq. (3):

$$W_C = W_{C_0} - M_C \cdot F_T \cdot 10^{-3} \int_0^t (C_{CO} + C_{CO_2}) dt \tag{3}$$

where: W_{C_0} is the initial amount of carbon (in mg) in the reactor (Eq. (4)); M_C is the atomic weight of carbon; F_T is the exit gas flow (in moles/s) (Eq. (5)); C_{CO} and C_{CO_2} are the concentrations of CO and CO_2 (in ppm), respectively, at time t.

$$W_{C_0} = M_C \cdot F_T \cdot 10^{-3} \int_0^\infty (C_{CO} + C_{CO_2}) dt \tag{4}$$

$$F_T = \frac{Q \cdot P}{R_g \cdot T} \tag{5}$$

In Eq. (5): Q is the total flow rate fed to the reactor (in m^3/s); P is the reactor pressure (in Pa); R_g is the universal gas constant (in Pa m^3/mol K); and T is the reactor temperature (K).

This method has been used in earlier works (e.g. [18,23]), for the analysis of the reactivity of different soot samples and soot surrogates.

5. Results and discussion

5.1. Reactivity soot-NO_2

Fig. 2 shows the time for the complete conversion of carbon at 500 °C for the interaction between NO_2 and the different soot samples obtained with the different fuels and engine operation modes considered.

As observed in Fig. 2, the engine operating conditions under which soot samples were generated have a direct influence on its oxidative reactivity with NO_2. This behavior agrees with previous studies on soot reactivity that point out the importance of the origin (specific combustion conditions) of the soot samples (e.g. [6,24]). Thus, different τ values are obtained depending on the operating mode of the diesel engine and the fuel fed. The sequence from most to least reactive soot is: Biodiesel_U9 + post > Biodiesel_U9 + p_{inj} > Diesel_U9 + p_{inj} > Biodiesel_U9 > HVO_U9 + p_{inj} ≈ GTL_U9 + p_{inj} > Diesel_U9 + post > HVO_U9 + post ≈ GTL_U9 + p

The influence of the engine operation mode is shown in Fig. 3, where the differences of the total carbon conversion time with respect to the urban U9 mode are represented. Independently on the fuel used, the time for the complete conversion of carbon (τ) is higher for the urban operation mode with the original engine calibration (U9) than for the other engine operation modes.

Thus, the U9 mode results in the formation of the least reactive soot. Both modifications applied to the urban mode (increased injection pressure or addition of a fuel post injection) lead to lower τ values and consequently higher reactivity. For designers of vehicle calibrations, these results indicate that there is margin for boosting the oxidation capability of soot trapped in the DPF, thus allowing for more efficient filter regenerations. Furthermore, with the exception of the biodiesel soot, the increased injection pressure (U9 + p_{inj}) mode shows the lowest τ values. Therefore, the general trend in reactivity, from the least to the most reactive soot, is U9 < U9 + post < U9 + p_{inj}. Only for biodiesel soot, the U9 + post mode shows a slightly lower τ value than the U9 + p_{inj}. In this case, the soot samples sorted, from the least to the most reactive, as: U9 < U9 + p_{inj} < U9 + post.

To analyze the influence of the fuel type on the reactivity of the soot formed with NO_2, the results obtained with the conventional diesel fuel are taken as reference for comparison (Fig. 4).

Considering the results obtained with the urban U9 mode, the diesel soot shows the highest time for the complete conversion of carbon, and therefore, among the four types of fuels analyzed, the diesel fuel results in the formation of a soot less reactive with NO_2. Both alternative paraffinic fuels, GTL and HVO, show higher reactivity than diesel soot. Biodiesel is, with significant difference, the fuel that generates the most reactive soot, as inferred from its τ value, which is much lower than for the rest of fuels analyzed. This behavior agrees with that observed for the other engine operation modes. Thus, the general trend in soot reactivity with NO_2 obtained as function of the fuel, from the least to the most reactive is: diesel < GTL ≈ HVO < biodiesel.

Moreover, Lapuerta et al. [16] observed that if the engine is fueled with paraffinic fuels or adding a post injection leads to a more reactive soot. This observation supports the results obtained in this work, as the soot from GTL and from HVO are more reactive than that derived from diesel fuel. Moreover using the post injection mode, higher reactivity is even achieved for the soot generated.

To analyze to what extent the soot-NO_2 interaction at 500 °C leads to an effective net nitrogen oxides reduction, Fig. 5 shows the NO_x reductions (%) achieved in the different experiments together with the NO and NO_2 conversions as function of the reaction time. The NO_x reduction values at any time are calculated from the data of the reactor inlet NO_2 concentration (before reaction) and the NO and NO_2 concentrations at the reactor outlet (after reaction).

Independently of the fuel and the engine operation mode used, the interaction of soot with NO_2 does not yield into a net NO_x reduction at diesel exhaust conditions, despite soot is consumed during this interaction. In all the cases, during the soot-NO_2 interaction at 500 °C, NO_2 is converted to NO.

5.2. Reactivity soot-O_2

As already indicated in the experimental section, the soot-O_2 experiments were performed with an initial fixed amount of soot which was first subjected to reaction with 5% O_2 at 500 °C. In this interaction, part of the initial soot sample was consumed, but not all. Afterwards, the remaining soot was subsequently subjected to reaction at an in-

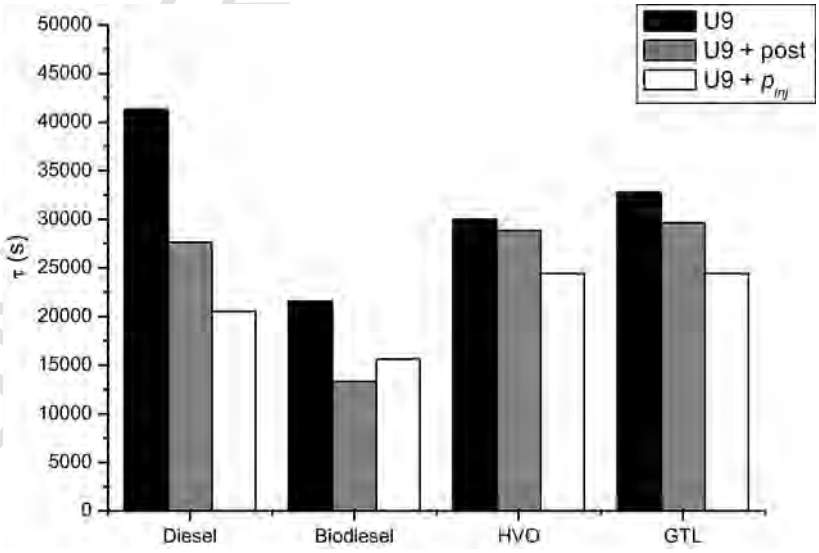

Fig. 2. Time for the complete conversion of carbon, τ, obtained in the reaction of NO_2 at 500°C with the different soot samples.

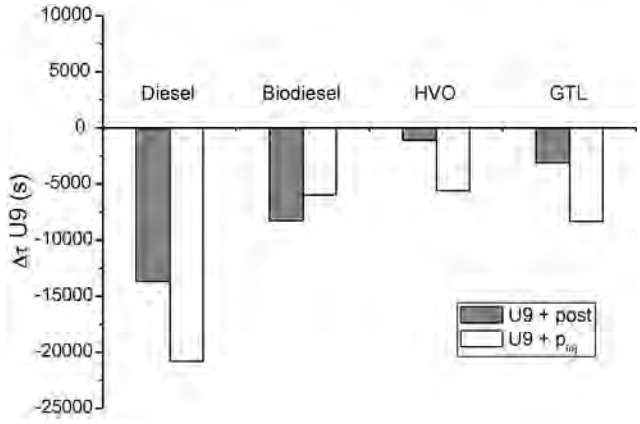

Fig. 3. Time for the complete conversion of carbon (τ) differences between the original calibration U9 mode and the variations in the injection settings: U9 + post and U9 + p_{inj}.

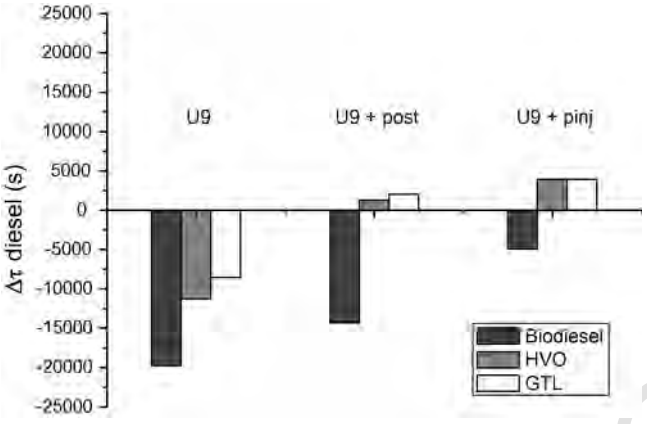

Fig. 4. Time for the complete conversion of carbon (τ) differences between the diesel fuel and the other fuels: biodiesel, HVO and GTL.

creased temperature (600 °C). After the run at 600 °C, when the reactor was removed from the electric furnace and dismantled, we verified that there was no soot remaining in the reactor. In addition, no signs of any black particles in the reactor bed were observed, which indicates the completeness of the soot oxidation reaction. This behavior denotes the heterogeneity of the soot samples with, at least, two soot fractions reacting at different temperatures, and agrees with previous studies on the reactivity of different carbonaceous materials with reactant gases: see, for instance, the work by Zolin et al. [25] with coal char, and the work by Abián et al. [24] with soot. Along with low-reactive fractions composed of graphitic lattices of C-atoms, other soot fractions are also present with more disordered lattices, with more crystalline defects or with different chemical functionalities attached to the edges of the carbon planes, which may be responsible for an enhanced reactivity. Under experimental conditions of limited temperature and restricted presence of oxidant species (500 °C and 5% O_2), soot oxidation may proceed only through the most reactive parts, while the rest needs a higher temperature (at fixed oxidant concentration) for a complete oxidation.

Considering the above described soot-O_2 experimental procedure, the total soot conversion at each temperature (500 and 600 °C), $X_{soot,i}(\%)$, was calculated through Eq. (6):

$$X_{soot,i}(\%) = \frac{W_{C_{react,i}}}{W_{C_{react,500}} + W_{C_{react,600}}} \cdot 100 \quad (6)$$

where subscript i denotes 500 or 600 °C and $W_{C_{react,i}}$ the total

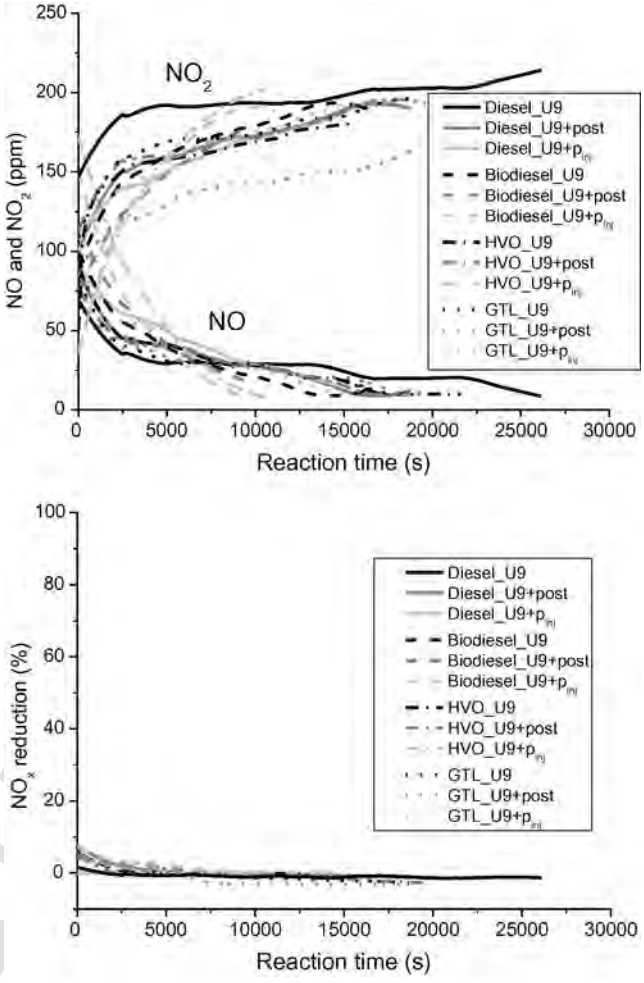

Fig. 5. NO and NO_2 conversion (ppm) and NO_x reduction (%) as function of the reaction time for the different soot samples. Soot-NO_2 interaction at 500 °C.

amount of carbon (in mg) consumed during the reaction at a given temperature. $W_{C_{react,i}}$ is calculated through Eq. (4).

In the same way, and considering that τ represents the time needed for the complete conversion of carbon, to analyze and compare the results, an equivalent tau, $\tau_{eq,i}$, has been defined, which takes into account the conversion of soot at each temperature. $\tau_{eq,i}$ is calculated through Eq. (7):

$$\tau_{eq,i} = \frac{\tau_i}{X_{soot,i}} \cdot 100 \quad (7)$$

where the subscript i denotes 500 or 600 °C, and τ_i is calculated through Eq. (1).

The results obtained at 500 °C are firstly analyzed. Fig. 6 shows the total soot conversion at 500 °C, $X_{soot,500}$ (%), and the corresponding equivalent tau values for the complete conversion of carbon ($\tau_{eq,500}$).

The sequence from the most to the least reactive soot in the soot-O_2 interaction at 500 °C is:

HVO_U9 + p_{inj} > GTL_U9 > Biodiesel_U9 > Biodiesel_U9 + post ≈ Biodiesel_U9 - GTL_U9 + post > HVO_U9 + post.

In view of the results shown in Fig. 6, there is not a clear tendency that relates the reactivity of soot with 5% O_2 at 500 °C, as function of the fuel used for the formation of soot and the engine operation mode. At 500 °C, except for diesel_U9 + p_{inj}_soot, biodiesel_U9_soot,

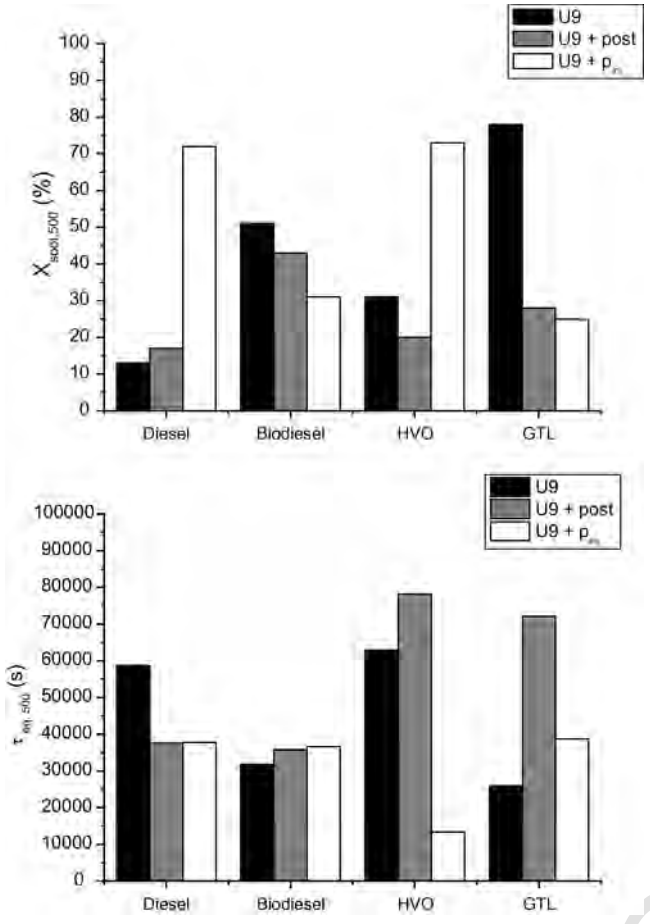

Fig. 6. Soot-O_2 interaction at 500 °C: total soot conversion, $X_{soot,500}$ (%), and equivalent tau values for the complete conversion of carbon, $\tau_{eq,500}$.

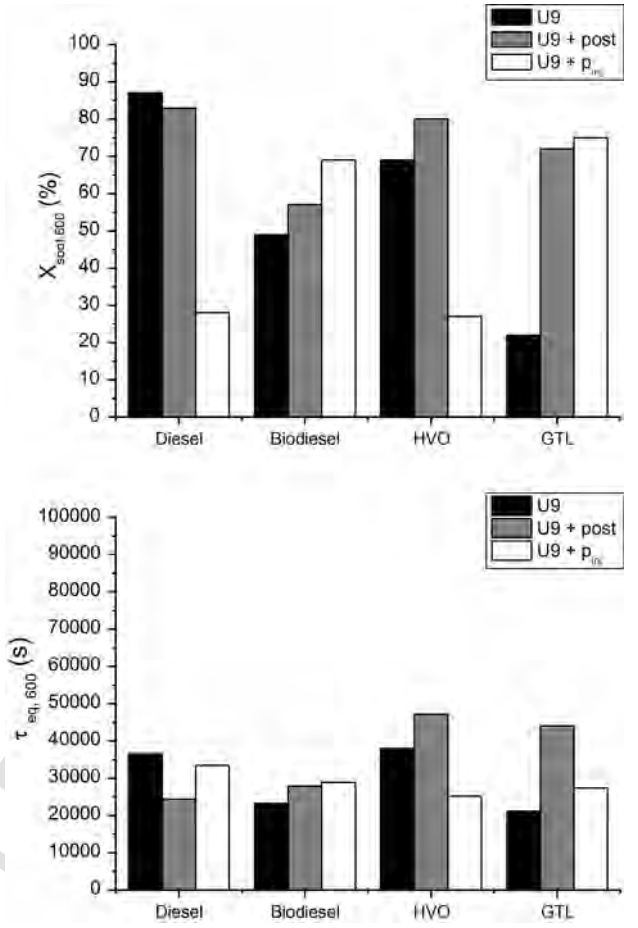

Fig. 7. Soot-O_2 interaction at 600 °C: total soot conversion, $X_{soot,600}$ (%), and equivalent tau values for the complete conversion of carbon ($\tau_{eq,600}$).

HVO_U9 + p_{inj}_soot and GTL_U9_soot, the total soot conversion is lower than 50%. This points to the fact that independently on the carbon consumption reaction rate, most of the soot sample remains within the bed, without reacting at 500 °C with 5% O_2. It is remarkable that the diesel_U9_soot shows the lowest soot conversion, with a $X_{soot,500}$ value lower than 15%.

Regarding the $\tau_{eq,500}$ values, the HVO_U9 + p_{inj}-soot and GTL_U9_-soot show the higher reactivity, whereas the HVO_U9 + post_soot and GTL_U9 + post_soot are the least reactive materials. Among all the soot samples analyzed, HVO_U9 + p_{inj}_soot is the most reactive soot and the one that shows higher $X_{soot,500}$ (%) values.

Next, the soot-5% O_2 reactivity at 600 °C is considered. Fig. 7 shows the total soot conversion at 600 °C, $X_{soot,600}$ (%), and the corresponding equivalent tau values for the complete conversion of carbon ($\tau_{eq,600}$).

In general, and despite the fact that the experiment at 600 °C is performed with the remaining soot from the soot-5% O_2 interaction at 500 °C, the higher the reaction temperature, the higher the reactivity of soot with O_2. At 600 °C, all the remaining soot reacts, and therefore the $X_{soot,600}$ shows the inverse trend to the one obtained at 500 °C. Under these conditions, the differences in reactivity ($\tau_{eq,600}$ values) among the different soot samples are less pronounced than at 500 °C, and again there is not a clear tendency that relates the reactivity of soot with 5% O_2, as function of the fuel used for the formation of soot and the engine operation mode.

In order to go deeper into the analysis of the interaction of soot with 5% O_2, selected soot samples were subjected to tests in a thermogravimetric analyzer (TGA – *Netzsch STA F1 Jupiter* thermogravimetric analyzer). The soot samples (around 1 mg) were oxidized in 5%O_2 (using N_2 as bath gas) during non-isothermal runs at 10 °C/min from room temperature to 700 °C. The initial soot sample mass and the heating rate were selected based on previous studies [24]. Fig. 8 shows the burning profile of Diesel_U9, Diesel_U9 + p_{inj}, HVO_U9 and HVO_U9 + p_{inj} soot.

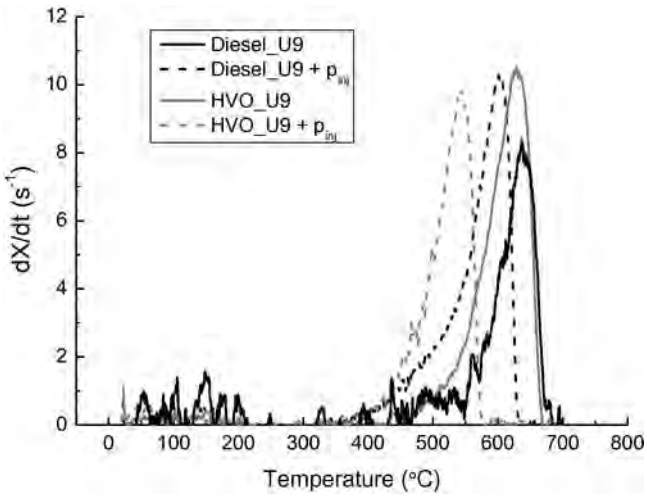

Fig. 8. Oxidation profile of soot samples: Diesel_U9, Diesel_U9 + p_{inj}, HVO_U9, HVO_U9 + p_{inj}. Data obtained from TGA experiments in 5 % O_2 atmosphere and a heating rate of 10 °C/min.

Considering the results shown in Fig. 8, HVO_U9 + p_{inj}-soot is the most reactive sample. It starts reacting at 350 °C, approximately, and shows the peak temperature, indicative of maximum burning rate (PT) at 540 °C. Diesel_U9 + p_{inj}-soot also starts to react at 350 °C, but with a lower consumption rate than HVO_U9 + p_{inj}-soot. At around 550 °C the slope of the burning rate profile is increased. The peak temperature is located at higher temperatures (PT = 600 °C) as well. Both HVO and Diesel soot samples obtained with the U9 engine operation mode start reaction at 450 °C, approximately. The consumption rate profile of the HVO_U9 soot is similar to Diesel_U9 + p_{inj}-soot, but the temperature window is shifted to higher temperatures. This way, the peak temperature is located at 630 °C. In the case of diesel_U9-soot, Fig. 8 shows two distinct peaks (apart from a first phase below 250 °C where water and other volatile compounds are removed): one at around 500 °C and the other one, which is significantly more relevant, at 635 °C. This result, obtained at limited oxygen availability, points to the presence of at least two phases in soot: a more reactive phase that reacts at lower temperatures, and a less reactive phase that reacts at higher temperatures, evidencing the heterogeneity of soot samples. Under more aggressive oxidizing conditions (for example, a higher oxygen concentration), all soot mass can be burnt with no distinction of two phases [16].

These soot burning profiles (Fig. 8) can be connected with the soot-O_2 interaction results at 500 °C (Fig. 6):

- The lower the peak temperature, indicative of maximum burning rate (Fig. 8), the lower the equivalent tau value needed for the complete conversion of carbon at 500 °C, $\tau_{eq,500}$ (Fig. 6), and consequently the higher the reactivity of the soot sample.
- The lower the onset temperature for the conversion of soot (Fig. 8), the higher the total soot conversion at 500 °C, $X_{soot,500}$ (Fig. 6).
- The higher the slope of the tangent line to the dX/dt curve at 500 °C (Fig. 8), the lower the equivalent tau value needed for the complete conversion of carbon at 500 °C, $\tau_{eq,500}$ (Fig. 6).

It is also interesting to note that the slope of the tangent line to the dX/dt curve at 600 °C can be directly related to the soot-O_2 interaction results at 600 °C. The soot samples analyzed show almost parallel tangent lines to their respective dX/dt curves at 600 °C (Fig. 8) and similar equivalent tau values for the complete conversion of carbon at 600 °C, $\tau_{eq,600}$ (Fig. 7); provided the PT is not located at temperatures lower than 600 °C. The HVO_U9 + p_{inj}-soot is fully consumed during the TGA test at temperatures lower than 600 °C, and, in agreement, the HVO_U9 + p_{inj}-soot shows a lower $\tau_{eq,600}$ value.

6. Conclusions

A study on the interaction of different soot samples with both 200 ppm of NO_2 at 500 °C and 5% vol. O_2 at 500 and 600 °C is presented. In general, both the given fuel (diesel, biodiesel, HVO or GTL) and the engine operation mode (U9, U9 + post, U9 + p_{inj}) used during the formation of soot significantly influences its further capacity to interact with NO_2 and O_2 at typical diesel exhaust conditions. However, the magnitude of the reduction of each soot sample depends on the reactant used, NO_2 or O_2.

6.1. Soot-NO2 interaction

On the one hand, when an urban engine operation mode is used, the soot generated from biodiesel or paraffinic fuels (HVO and GTL) is more reactive than the one generated by the diesel fuel, highlighting the potential of the alternative fuels to minimize soot emissions in diesel engines. For all fuels, both modifications applied to the urban mode (increased injection pressure or addition of a fuel post injection) led to higher soot reactivity.

On the other hand, the reduction of soot is not accompanied by a net reduction of NO_x. During the reaction, the NO_2 is converted to NO, keeping the total NO_x concentration constant and equal to initial concentration of NO_2.

6.2. Soot-5%O2 interaction

The oxygen concentrations that can be typically found at diesel engine exhaust (i.e. 5% O_2) are not enough to fully oxidize the present soot samples at 500 °C. The extent of the soot-5% O_2 interaction at 500 °C depends strongly on the characteristics of the soot sample. At the urban engine operation mode (U9), the soot generated with the alternative fuels shows higher carbon conversion values than the one generated with the diesel fuel. The soot sample from diesel and the urban U9 mode shows the lowest soot conversion at 500 °C, and consequently both modifications applied to the urban mode (increased injection pressure or addition of a fuel post injection) led to higher soot conversions.

Therefore, it can be concluded that both the fuel and engine operating mode have a significant impact on the subsequent reactivity of the soot generated, which can be used to develop strategies to minimize the accumulation of this pollutant in the particulate filter of diesel engines.

Acknowledgements

The authors express their gratitude to Aragón Government and European Social Fund (GPT group), and to Spanish Ministry of Economy and Competitiveness and FEDER (Projects CTQ2015-65226 and ENE2013-48602-C3-1-R) for financial support. Jesús Sánchez – Valdepeñas acknowledges to Junta de Comunidades de Castilla – La Mancha for the fellowship.

References

[1] World Health Organization (WHO), International Agency for Research on Cancer. IARC: diesel exhaust carcinogenic, No 213; 2012.
[2] Intergovernmental Panel on Climate Change/Working Group I (IPCC/WG1), The Physical Science Basis, Cambridge University Press, Cambridge, UK, 2013.
[3] Directive 136/2014/CE of the European Parliament and of the Council.
[4] I.P. Kandylas, O.A. Haralampous, G.C. Koltsakis, Diesel soot oxidation with NO_2: engine experiments and simulations, Ind Eng Chem Res 41 (2002) 5372–5384.
[5] C.J. Tighe, M.V. Twigg, A.N. Hayhurst, J.S. Dennis, The kinetics of oxidation of diesel soots by NO_2, Combust Flame 159 (2012) 77–90.
[6] A. Messerer, R. Niessner, U. Pöschl, Comprehensive kinetic characterization of the oxidation and gasification of model and real diesel soot by nitrogen oxides and oxygen under engine exhaust conditions: Measurement, Langmuir-Hinshelwood, and Arrhenius parameters, Carbon 44 (2006) 307–324.
[7] M. Schejbal, J. Stepanek, M. Marek, P. Koci, M. Kubicek, Modelling of soot oxidation by NO_2 in various types of diesel particulate filters, Fuel 89 (2010) 2365–2375.
[8] H. Muckenhuber, H. Grothe, The heterogeneous reaction between soot and NO_2 at elevated temperature, Carbon 44 (2006) 546–559.
[9] K. Leistner, A. Nicolle, P. Da Costa, Detailed kinetic analysis of soot oxidation by NO_2, NO, and NO + O_2, J Phys Chem C 116 (2012) 4642–4654.
[10] J.O. Müller, B. Frank, R.E. Jentoft, R. Schlögl, D.S. Su, The oxidation of soot particulate in the presence of NO_2, Catal Today 191 (2012) 106–111.
[11] F. Arens, L. Gutzwiller, U. Baltensperger, H. Gäggeler, M. Ammann, Heterogeneous reaction of NO_2 on diesel soot particles, Environ Sci Technol 35 (2001) 2191–2199.
[12] S. Lelièvre, Y. Bedjanian, G. Laverdet, G. Le Bras, Heterogeneous reaction of NO_2 with hydrocarbon flame soot, J Phys Chem A 108 (2004) 10807–10817.
[13] D.G. Aubin, J.P.D. Abbatt, Interaction of NO_2 with hydrocarbon soot: focus on HONO yield, surface modification, and mechanism, J Phys Chem A 111 (2007) 6263–6273.
[14] M. Lapuerta, J. Rodríguez Fernández, F. Oliva, Effect of soot accumulation in a diesel particle filter on the combustion process and gaseous emissions, Energy 47 (2012) 543–552.
[15] J.D. Martínez, J. Rodríguez-Fernández, J. Sánchez-Valdepeñas, R. Murillo, T. García, Performance and emissions of an automotive diesel engine using a tire pyrolysis liquid blend, Fuel 115 (2014) 490–499.

[16] M. Lapuerta, J. Rodríguez-Fernández, J. Sánchez-Valdepeñas, M.S. Salgado, Multi-technique analysis of soot reactivity from conventional and paraffinic diesel fuels, Flow Turbulence Combust 96 (2016) 327–341.
[17] M. Guerrero, M.P. Ruiz, M.U. Alzueta, R. Bilbao, A. Millera, Pyrolysis of eucalyptus at different heating rates: studies of char characterization and oxidative reactivity, J Anal Appl Pyrolysis 74 (2005) 307–314.
[18] C. Arnal, M.U. Alzueta, A. Millera, R. Bilbao, Experimental and kinetic study of the interaction of commercial soot with NO at high temperature, Combust Sci Technol 184 (2012) 1191–1206.
[19] M. Abián, A. Millera, R. Bilbao, M.U. Alzueta, Interaction soot-SO_2. Experimental and kinetic analysis, Combust Sci Technol 188 (2016) 482–491.
[20] M. Lapuerta, J.J. Hernández, F. Giménez, Evaluation of exhaust gas recirculation as a technique for reducing diesel engine NO_x emissions, Proc. Inst. Mech. Eng., Part D: J. Automob. Eng. 214 (2000) 85–93.
[21] O. Levenspiel, Ingeniería de las reacciones químicas, 2nd ed., Reverté SA, Barcelona, 2002.
[22] B.R. Stanmore, J.F. Brilhac, P. Gilot, The oxidation of soot: a review of experiments, mechanisms and models, Carbon 39 (2001) 2247–2268.
[23] C. Arnal, M.U. Alzueta, A. Millera, R. Bilbao, Influence of water vapor addition on soot oxidation at high temperature, Energy 43 (2012) 55–63.
[24] M. Abián, A.D. Jensen, P. Glarborg, M.U. Alzueta, Soot reactivity in conventional combustion and oxy-fuel combustion environments, Energy Fuels 26 (2012) 5337–5344.
[25] A. Zolin, A.D. Jensen, P.A. Jensen, K. Dam-Johansen, Experimental study of char thermal deactivation, Fuel 81 (2002) 1065–1075.